

Photoluminescence polarization in strained GaN/AlGaIn core/shell nanowires

This article has been downloaded from IOPscience. Please scroll down to see the full text article.

2012 Nanotechnology 23 325701

(<http://iopscience.iop.org/0957-4484/23/32/325701>)

View [the table of contents for this issue](#), or go to the [journal homepage](#) for more

Download details:

IP Address: 129.6.196.30

The article was downloaded on 19/07/2012 at 01:26

Please note that [terms and conditions apply](#).

Photoluminescence polarization in strained GaN/AlGaIn core/shell nanowires

G Jacopin¹, L Rigutti^{1,2}, S Bellei¹, P Lavenus¹, F H Julien¹,
A V Davydov³, D Tsvetkov³, K A Bertness⁴, N A Sanford⁴, J B Schlager⁴
and M Tchernycheva¹

¹ Institut d'Electronique Fondamentale UMR CNRS 8622, University Paris Sud, 91405 Orsay, France

² Groupe de Physique des Matériaux UMR CNRS 6634, University of Rouen, 76801 St Etienne du Rouvray, France

³ MML, NIST, Gaithersburg, MD 20899, USA

⁴ PML, NIST, Boulder, CO 80305, USA

E-mail: gwenole.jacopin@u-psud.fr

Received 12 April 2012, in final form 26 June 2012

Published 17 July 2012

Online at stacks.iop.org/Nano/23/325701

Abstract

The optical polarization properties of GaN/AlGaIn core/shell nanowire (NW) heterostructures have been investigated using polarization resolved micro-photoluminescence (μ -PL) and interpreted in terms of a strain-dependent $6 \times 6 \mathbf{k} \cdot \mathbf{p}$ theoretical model. The NW heterostructures were fabricated in two steps: the Si-doped n-type *c*-axis GaN NW cores were grown by molecular beam epitaxy (MBE) and then epitaxially overgrown using halide vapor phase epitaxy (HVPE) to form Mg-doped AlGaIn shells. The emission of the uncoated strain-free GaN NW core is found to be polarized perpendicular to the *c*-axis, while the GaN core compressively strained by the AlGaIn shell exhibits a polarization parallel to the NW *c*-axis. The luminescence of the AlGaIn shell is weakly polarized perpendicular to the *c*-axis due to the tensile axial strain in the shell.

(Some figures may appear in colour only in the online journal)

1. Introduction

Ultraviolet (UV) nitride-based light emitting diodes (LEDs) are attracting considerable attention due to their numerous potential applications, including water purification [1], document authentication, medical diagnostics and phototherapy [2]. However, planar UV LEDs have a lower efficiency than standard blue LEDs [3] due to material and technological issues such as a high density of structural defects [4], difficulties with efficient p-doping of AlGaIn alloys with high Al content [5], issues related to the internal electric field in the quantum wells [6] and problems of light extraction efficiency [7], partly related to the unfavorable light polarization parallel to the *c*-axis in AlGaIn layers with Al content above 12% [8]. Nitride core/shell NWs have been intensively studied as building blocks for novel optoelectronic devices such as solar cells [9], LEDs [10–12] or optically pumped nanowire lasers [13]. In the context of LEDs, a quasi-1D geometry is advantageous since NWs are

essentially defect-free [14, 15]. This geometry also provides more flexibility in the design of the active region, by making use of non-polar NW facets. Finally, it allows the possibility of emission polarization engineering by tuning the thicknesses and chemical composition of the GaN/AlGaIn heterostructure.

The optical polarization of nitride nanowire photoluminescence has been studied by different authors [16–18]. It has been shown that the polarization properties can be affected by the nanowire elongated shape [17, 19]. However, to our knowledge, the influence of the strain state on the polarization properties of a core–shell nanowire has not been investigated yet.

In this work, we report on the optical properties of n-GaN/p-AlGaIn core/shell nanowires. These NWs represent a first building block for a complete UV LED structure based on n-GaN/n-AlGaIn/p-AlGaIn core–multishell NWs. The NW heterostructures are grown in two steps using MBE for the Si-doped n-GaN core and HVPE for the Mg-doped AlGaIn shell. The emission properties of the

individual core/shell structures are investigated by position- and polarization-resolved μ -PL at low temperature. The emission of the uncoated strain-free GaN NW core is polarized perpendicular to the c -axis, while the GaN core compressively strained by the AlGaIn shell exhibits a polarization parallel to the NW c -axis. The luminescence of the AlGaIn shell is weakly polarized perpendicular to the c -axis due to the tensile axial strain in the shell. These polarization properties can be straightforwardly interpreted by considering the effects of uniaxial strain along the c -axis on the electronic band structure of GaN and AlGaIn in the framework of a $6 \times 6 \mathbf{k} \cdot \mathbf{p}$ model [20].

2. Sample fabrication and microstructure

Si-doped n-type GaN NWs were grown along the wurtzite c -axis on Si(111) substrate by plasma-assisted MBE. Details on the growth procedure are described in [21]. The NWs lengths were uniform at $15 \pm 0.1 \mu\text{m}$, while their diameters ranged from 50 to 500 nm. In a second step, HVPE growth was employed to form Mg-doped AlGaIn shells over the MBE-grown GaN⁵ NWs. The HVPE growth conditions were similar to those described in [22] for fabricating p-GaN shells over MBE-grown n-GaN cores. The choice of the HVPE technique for shell overgrowth is motivated by the limited capacity of MBE to achieve core/shell growth in the same process, more efficient p-doping in HVPE process [22], and better compositional uniformity of $\text{Al}_x\text{Ga}_{1-x}\text{N}$ alloys in the whole range of x from 0 to 1. The thickness of the conformally deposited epitaxial shells on the GaN NW sidewalls was in the range from 50 to 700 nm. Figure 1 shows an array of vertically-aligned core/shell NWs. During the shell growth for some closely spaced GaN NWs, shadowing effects resulted in only partial AlGaIn shell formation. The inset in figure 1 shows an example of such a non-uniform coating, where an AlGaIn shell has only been formed over the top $5 \mu\text{m}$ of the NW.

The Al content in AlGaIn shells was determined by x-ray diffraction (XRD) measurements and energy dispersive x-ray spectroscopy (EDX). XRD was performed on the core/shell NW arrays using a Scintag D-500 powder diffractometer⁶ with Cu $K\alpha_1$ radiation, while elemental analysis was done on individual core/shell NWs using an Oxford Instruments EDX detector attached to a Hitachi S4700 field emission scanning electron microscope (FE-SEM).

The XRD pattern shown in figure 2 reveals the presence of 000 l reflections from the core/shell structures, confirming that AlGaIn forms conformal epitaxial shells over the vertically-aligned GaN NWs. The XRD pattern was used to estimate the Al content in the AlGaIn shell although the XRD analysis does not allow separation of the effect of strain from that of composition. As a first approximation for the Al content estimation the strain in the AlGaIn shell was

⁵ For comparison with the previously published data [21], the growth runs were 'C023' for the GaN core and 'N173' for the AlGaIn shell.

⁶ Any mention of commercial products in this article is for information only; it does not imply recommendation or endorsement by the NIST.

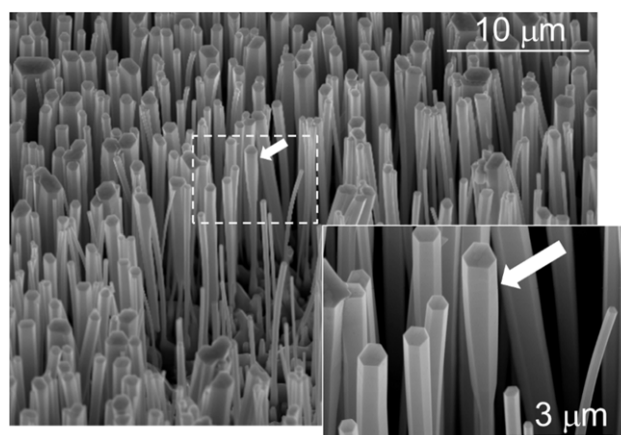


Figure 1. (a) Tilted SEM view of the GaN-core/AlGaIn-shell nanowire heterostructures on Si substrate. The inset shows a magnified view of the cone-shaped nanowire due to AlGaIn shell thickening towards the NW top.

neglected. Deconvolution of the broad $\text{Al}_x\text{Ga}_{1-x}\text{N}$ component from the main 0004 GaN peak in the inset of figure 2 (at $2\theta = 73.4^\circ$) allows measurement of the c -lattice parameter and gives an estimation of the $\text{Al}_x\text{Ga}_{1-x}\text{N}$ composition centered around $x = 0.23 \pm 0.07$. The shoulder at $2\theta = 74.8^\circ$ with the two-orders of magnitude lower intensity is assigned to $\text{Al}_x\text{Ga}_{1-x}\text{N}$ with $x = 0.62 \pm 0.07$. The uncertainty of 7 at.% is derived from the x versus c -parameter calibration, produced in our previous study of AlGaIn films (calibration curves not shown) [23].

To correlate these two distinct $\text{Al}_x\text{Ga}_{1-x}\text{N}$ compositions with the core/shell microstructure, EDX analysis was performed on individual NWs detached from the substrate. The EDX analysis revealed that the $\text{Al}_x\text{Ga}_{1-x}\text{N}$ shell atop the GaN NW is considerably richer in Al than on the NW sidewalls. Typical EDX spectra together with the corresponding SEM image of the analyzed core/shell NW are shown in figure 3. The composition x measured at the top of the shell is 0.54 whereas on the sidewalls of the shell it is only 0.27. The statistical error of measuring Al content by EDX did not exceed $\Delta x = \pm 0.05$.

For the NW base the absence of an Al signal confirms the absence of the AlGaIn coating in this region. It should be noted that the EDX analysis was conducted under a low acceleration voltage of 5 keV to ensure that the probe penetration depth did not exceed the actual AlGaIn shell thickness; applying Casino 2.42 simulation [24], the calculated excitation depth did not exceed $100 \pm 20 \text{ nm}$ for the $\text{Al}_{0.2}\text{Ga}_{0.8}\text{N}$ composition, while the actual shell thickness in spots '2' and '3' in figure 3 was estimated from SEM to be 150 to 200 nm. Nevertheless, in view of the possible contribution of a Ga signal from the GaN core to the overall Ga EDX peak, the evaluated EDX compositions should be considered as low-end estimates of the Al content for this particular NW. Taking into account wire-to-wire composition fluctuations, the EDX results are in reasonable agreement with the composition values deduced from the XRD in figure 2.

From the XRD scans on the randomly oriented GaN NWs before and after AlGaIn shell coating (not shown), we

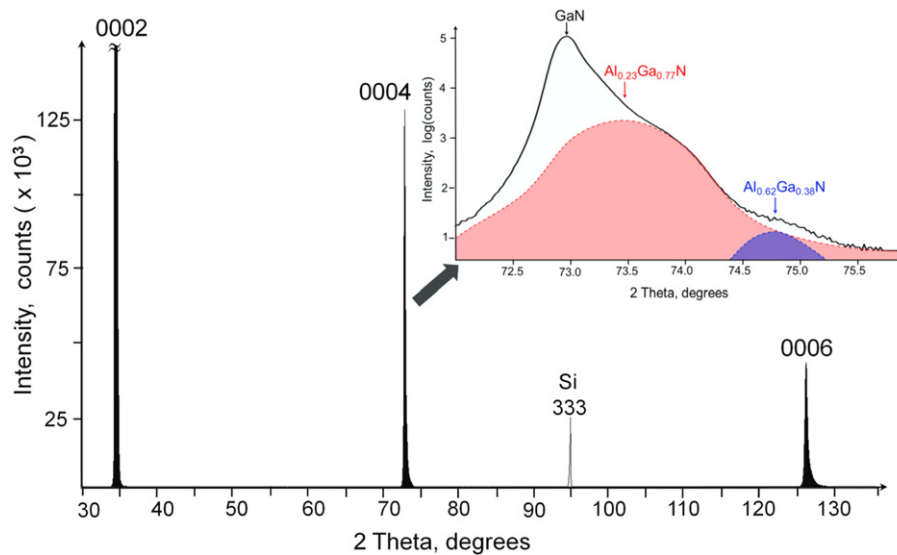


Figure 2. XRD pattern of the core/shell heterostructure NW ensemble shown in figure 1. The $000l$ reflections from the GaN/AlGa $_x$ N NW arrays dominate the pattern. The inset shows a deconvolution of the 0004 reflection into the GaN main peak (peak profile is not shown) and two Al $_x$ Ga $_{1-x}$ N peaks corresponding to Al-poor (red indicated peak with x near 0.23) and Al-rich (blue indicated peak with x near 0.62) compositions.

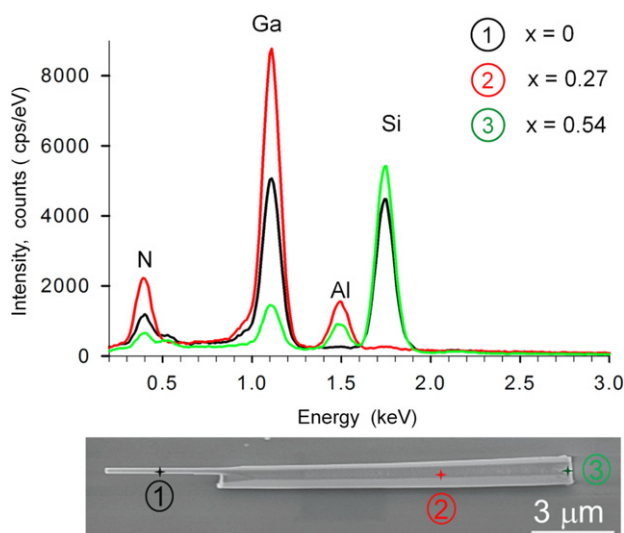


Figure 3. EDX spectra (top figure) measured in three spots of a typical core/shell NW (SEM image shown in the bottom figure) used for PL study. The Al $_x$ Ga $_{1-x}$ N composition for each spot is $x = 0, 0.27$ and 0.54 , respectively. Note the absence of AlGa $_x$ N coating at the NW base (left). The strong Si signal in the EDX spectra 1 and 3 arises from the underlying Si substrate.

have estimated the compressive strain induced by the AlGa $_x$ N shell in the GaN NW cores. For these measurements, NWs that were still attached to the substrate were mechanically disturbed to disrupt their vertical alignment. The induced random orientation of NWs allowed one to observe all GaN diffraction peaks, including the asymmetric reflections. The 2Θ Cu K α_1 range from 32° to 127° was used to refine the GaN lattice parameters by the least-squares method in Jade 5.0 (Materials Data Inc., Livermore, CA). The corresponding GaN lattice parameters were calculated as follows: $a_0 =$

$3.1908 \pm 0.0012 \text{ \AA}$, $c_0 = 5.1842 \pm 0.0001 \text{ \AA}$ for uncoated NWs, and $a_1 = 3.1890 \pm 0.0015 \text{ \AA}$, $c_1 = 5.1813 \pm 0.0002 \text{ \AA}$ for the GaN peak of the AlGa $_x$ N shell coated NWs. From this analysis, while the shell-induced compression in the a -direction was found to be statistically insignificant due to the large experimental uncertainty, the c -compression value was evident, with $(c_1 - c_0)/c_0 = -5.6 \times 10^{-4}$. It should be noted that this value averages the strain in the whole nanowire ensemble, while the strain of individual nanowires can deviate from this value, as was found from the optical measurements in section 3. Notably, it was not possible to use XRD to extract strain values in the AlGa $_x$ N shells due to the absence of the ‘lattice parameters versus Al content’ calibration curve for strain-free AlGa $_x$ N alloys. An uncertainty in the peak position for unstrained material made it impossible to deconvolute the effect of strain from that of alloy composition on the absolute location of AlGa $_x$ N peaks.

3. Optical spectroscopy

For the μ -PL studies, wires were detached from their growth substrate by means of ultrasonic agitation in ethanol and then dispersed on a patterned Si substrate with alignment marks. Position and polarization resolved μ -PL spectra were recorded at low temperature around 5 K by exciting the wire with a cw frequency doubled Ar $^{++}$ ion laser operating at 244 nm. The laser was focused onto a spot diameter of $2 \mu\text{m}$ by a UV objective microscope with 0.4 numerical aperture. The position resolved μ -PL spectral image was obtained by scanning the laser spot along the axial direction of the wire by means of an automated X–Y piezoelectric stage. In order to analyze the polarization of the emission, a linear polarizer was placed at the entrance of the spectrometer. For different positions along the wire, series of spectra were collected at different angles of the polarizer, which was varied over the

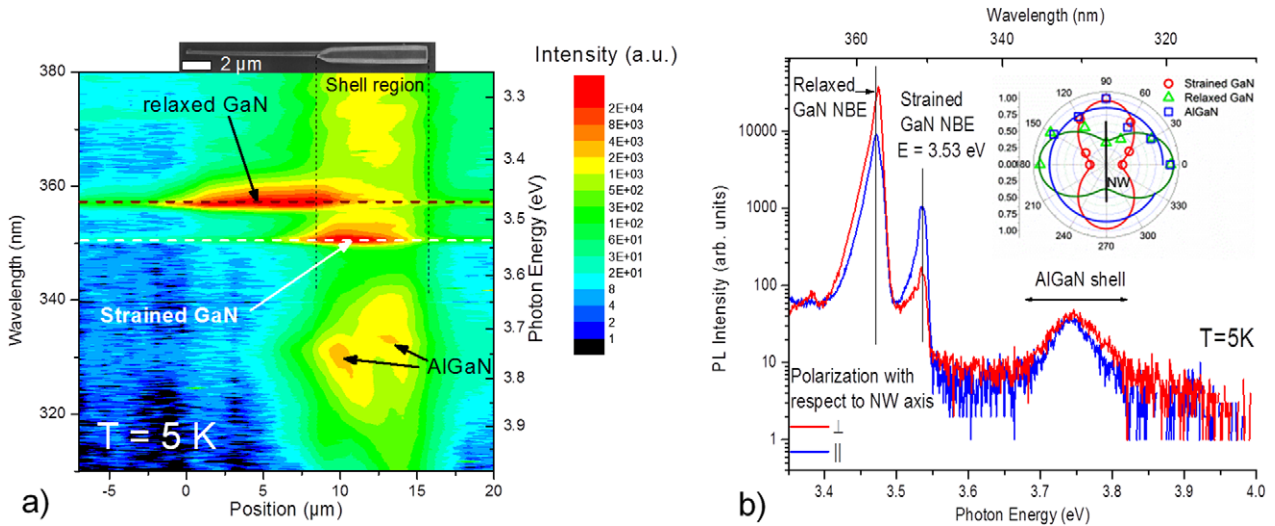


Figure 4. (a) μ -PL line scan of a single core/shell wire (the wire SEM image is shown at the top). (b) μ -PL spectra at different polarization at $T = 5$ K. Inset—normalized polarization diagram for the three different peaks: relaxed GaN at 3.47 eV (green), strained GaN at 3.53 eV (red) and AlGaIn peak around 3.75 eV (blue).

interval 0° to 180° with a 15° step size. The response of the system to horizontally or vertically directed light was calibrated using UV light from different unpolarized sources with energies in the range 3.3–3.8 eV. The orientation and the position of the studied wires with respect to the alignment crosses were determined by means of a visualization system consisting of LED illumination and a CCD camera. The morphology of the wires was analyzed using an SEM. The alignment marks were used to locate the wires under study and to assess their orientation for the polarization analysis.

We now discuss the emission properties on a typical single wire. A μ -PL line scan along the wire axis is reported in figure 4(a) together with the corresponding SEM image. At the base of the wire, we observe the emission related to the donor-bound X_A exciton of relaxed GaN (D^0X_A) at 3.47 eV [25]. On the top of the wire, where the core/shell structure is located, two main contributions appear in the spectrum. The first peak centered around 3.53 eV is attributed to the strained GaN [16, 17] and a band at higher energy 3.7–3.8 eV is ascribed to the AlGaIn shell. These attributions will be confirmed in section 4 by the polarization analysis and comparison with theoretical predictions. In addition, we observed a weak sub-bandgap emission below 3.4 eV related to donor–acceptor pair (DAP) transitions in AlGaIn [26] or to interface defects [27].

The μ -PL spectra of figure 4(b) were recorded for \parallel (electric field \parallel to c -axis) and \perp (electric field \perp to c -axis) polarizations at 5 K in the intermediate region of the wire, where both core and core/shell contributions are present near the 13 μ m position in figure 4(a). By rotating the polarization from \parallel to \perp , we observed that the relative intensity of the peaks changes. The polarization ratio is defined as:

$$P = \frac{I_{\perp} - I_{\parallel}}{I_{\perp} + I_{\parallel}}$$

where I_{\parallel} and I_{\perp} are the integrated PL intensities for \parallel and \perp polarization, respectively. The peak related to the near band

edge of relaxed GaN emission is maximal when the electric field is perpendicular to the c -axis with a polarization ratio of 0.62. The peak related to strained GaN is polarized parallel to the c -axis with a polarization ratio of -0.73 . The PL arising from the AlGaIn shell is slightly polarized perpendicular to the c -axis with a small polarization ratio of 0.09. The polarization diagrams of these three components are shown in the inset of figure 4(b). The polarization angular dependence can be well fitted by a cosine-squared law.

4. Theoretical considerations and discussion

The polarization properties are related to the valence band ordering and the selection rules of the related excitonic transitions. Thus, to predict the polarization behavior of the PL of a core/shell wire, we have calculated the valence band electronic states at the center of the Brillouin zone using a $6 \times 6 \mathbf{k} \cdot \mathbf{p}$ model including spin–orbit interaction under the quasi-cubic approximation [20]. To take into account the stress effects, we have used the Bir–Pikus approach as in [28]. The band structure parameters have been taken in agreement with Ghosh *et al* [28] for GaN and with Vurgaftman and Meyer [29] for AlN. All parameters for AlGaIn are deduced by a linear interpolation between those of GaN and AlN, except for the bandgap, where a bowing parameter of 1 eV has been used [30]. The diagonalization method to determine the three excitonic transition energies is explained in detail in Ghosh *et al* [28]. The polarization ratio is then derived from the eigenstates of the Hamiltonian, assuming Boltzmann's statistics for the population of exciton states.

In the case of nanowires, the polarization properties of the emission are determined not only by the excitonic selection rules, but also by the dielectric index contrast between the nanowire and the surrounding medium [31]. However, possible influence of the nanowire shape on the polarization properties, which is very strong in GaN nanowires with a

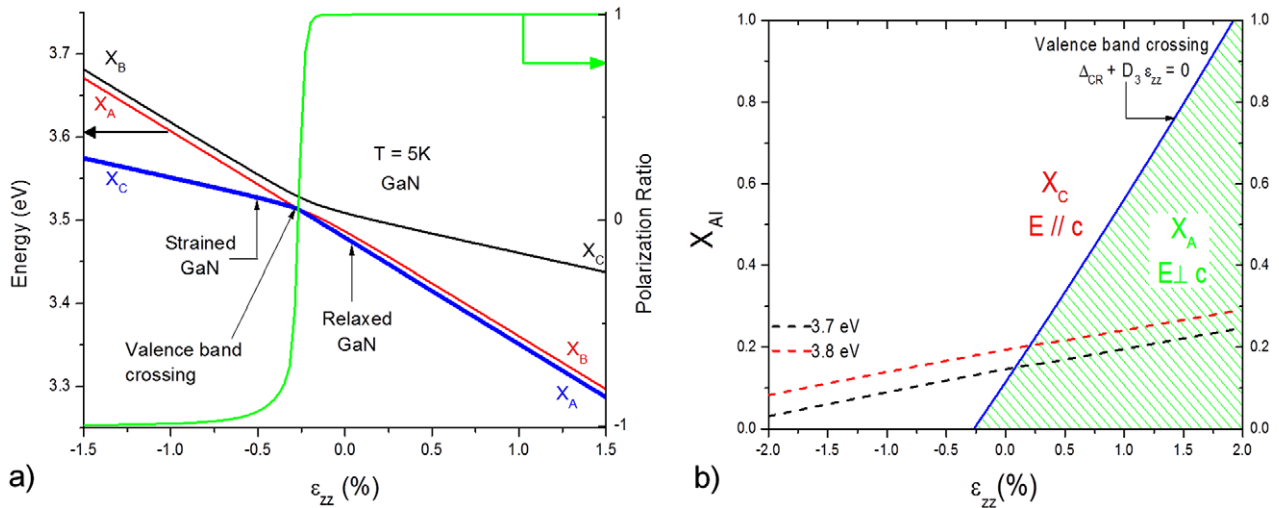


Figure 5. (a) Calculated excitonic transition energies as a function of uniaxial strain in GaN and polarization ratio of GaN near-band-edge emission (green line) depending on uniaxial strain along the c -axis for $T = 5\text{ K}$. (b) PL polarization diagram as a function of Al concentration and uniaxial strain. The dashed lines correspond to the experimentally observed emission energy of 3.7 eV and 3.8 eV, respectively. A schematic diagram of a AlGaIn/GaN core/shell nanowire showing z -axis orientation is depicted in the inset.

small diameter [32], is expected to be negligible in the present case because the wires have a diameter above 100 nm [31]. Therefore, the polarization properties of AlGaIn/GaN NWs can be completely understood in terms of valence band ordering.

As has been shown both theoretically and experimentally [17, 33, 34], in the case of AlGaIn/GaN core/shell wires, the in-plane strain is typically about ten times smaller than the axial strain and the optical properties are governed by the axial strain. This is also confirmed by the XRD measurements on randomly oriented NWs with statistically significant c -axial compressive strain in the GaN core as determined in section 1. As for the AlGaIn shell, the outer shell thickness in our case exceeds the critical value for a coherently strained nanowire [35] and we expect a partial strain relaxation in the shell via dislocations. The residual strain is assumed to remain uniaxial. The exact strain value in the AlGaIn shell is very difficult to extract from microstructural analysis due to absence of the 'lattice parameters versus Al content' calibration curve for strain-free AlGaIn alloys, which is further complicated by the compositional variation in the shells, both from wire to wire and within the same wire. In the following, we neglect the in-plane strain in the polarization analysis, i.e. $\epsilon_{yy} + \epsilon_{xx} \approx 0$ [33], taking z as the c -axis (the axis orientation is illustrated in the inset to figure 5(b) showing a schematic of a nanowire). The theoretical dependence of the three exciton energies in GaN on the uniaxial strain along z is shown in figure 5(a).

As observed in figure 5(a), at zero strain, the lowest excitonic transition is the X_A exciton, i.e. the topmost valence band is the A band. For increasing uniaxial compressive strain, A and C bands are getting closer and the crossing occurs at $\epsilon_{zz} \approx -0.27\%$. The band crossing corresponds to the change of symmetry of the uppermost valence band from Γ_9 to Γ_7 [36]. A further increase of ϵ_{zz} values leads to a stronger C and A band separation.

As shown by Chuang *et al* [20], the excitonic transition implies each valence band and is characterized by a specific polarization: the X_A excitonic transition is polarized perpendicular to the c -axis whereas the X_C excitonic transition is polarized parallel to the c -axis. Hence, at low temperature, the polarization ratio changes rapidly around band crossing. As shown in figure 5(a), the polarization ratio for GaN near-band-edge emission changes its sign for axial strain around $\epsilon_{zz} \approx -0.27\%$ due to the valence band re-ordering. As seen in figure 5(a), the PL arises from X_C excitons for $\epsilon_{zz} < -0.27\%$ (strained GaN) and X_A excitons for $\epsilon_{zz} > -0.27\%$ (relaxed GaN).

In the case of ternary AlGaIn alloy, the band crossing between the A and C valence bands occurs for a value of strain that depends on the Al content. Following the $6 \times 6 \mathbf{k} \cdot \mathbf{p}$ theory, we can derive the condition of band crossing when $\epsilon_{xy} = \epsilon_{yz} = \epsilon_{zx} = 0$:

$$\Delta_{cr} + D_3 \epsilon_{zz} + D_4 (\epsilon_{xx} + \epsilon_{yy}) = 0$$

where Δ_{cr} is the crystal field splitting, D_3 and D_4 are deformation potentials.

In the approximation of negligible in-plane strain, this gives the following simplified condition:

$$\Delta_{cr}(X_{Al}) = -D_3(X_{Al}) \epsilon_{zz}$$

where $\Delta_{cr}(X_{Al})$ and $D_3(X_{Al})$ are functions of the Al content which change linearly from $\Delta_{cr}(\text{GaIn})$ (resp. $D_3(\text{GaIn})$) for $x = 0$ to $\Delta_{cr}(\text{AlIn})$ (resp. $D_3(\text{AlIn})$) for $x = 1$.

Figure 5(b) shows the dominant exciton [37] for wurtzite $\text{Al}_x\text{Ga}_{1-x}\text{N}$ under uniaxial strain ϵ_{zz} as a function of Al content. The solid line shows the valence band crossing. From this diagram it is clear that the perpendicular polarization of $\text{Al}_x\text{Ga}_{1-x}\text{N}$ ($x > 0.12$) X_A emission anticipates a tensile strain in the AlGaIn shell.

The emission of relaxed GaN originating from the excitonic ($D^\circ X_A$) transition is predicted to be polarized

perpendicular to the c -axis in agreement with measurements. For strained GaN, our calculations predict that the observed PL energy at 3.53 eV corresponds to a strain state of GaN core around $\varepsilon_{zz} = -0.55\%$. For this value, we expect a negative polarization ratio in agreement with the PL measurements. Since the observed AlGaIn emission is almost unpolarized, the diagram of figure 5(b) shows that the AlGaIn strain is close to the valence band crossing line. Taking into account the observed AlGaIn peak PL energy of 3.7–3.8 eV, we estimate the Al content and the relative strain of the $\text{Al}_x\text{Ga}_{1-x}\text{N}$ shell as $x_{\text{Al}} \approx 15\text{--}22\%$ and $\varepsilon_{zz} \approx 0.20\%$, respectively. The estimated Al composition is compatible with the value deduced from the XRD and EDX measurements. Notably, the average strain value along the c axis in the GaN core found from XRD ($\varepsilon_{zz} \sim 0.056\%$) does not coincide with the $\varepsilon_{zz} \sim 0.55\%$ value found from μPL on a single wire. This discrepancy is most likely related to the fact that XRD has been performed on the whole ensemble of wires. In this case, the 5 μm thick GaN wetting layer on Si substrate as well as the uncovered wire bases and wires with thinner AlGaIn shells also contribute to the position and broadening of the XRD peak for the strained GaN core. The shown μPL results, on the other hand, refer to a single wire with a thick AlGaIn shell.

5. Conclusions

The polarization properties of wurtzite AlGaIn/GaN core-shell nanowires have been investigated by means of spatially resolved polarization-dependent micro-photoluminescence. The experimental results are interpreted in terms of the strain-induced valence band crossing determined from the $6 \times 6 \mathbf{k} \cdot \mathbf{p}$ theory. In particular, we observe that the polarization of GaN photoluminescence changes from perpendicular to the c -axis for strain-free nanowire base part to parallel to the c -axis for compressively strained GaN core. The emission of AlGaIn shell is weakly polarized perpendicular to the c -axis. This result shows that strain engineering in nanowire-based core/multishell n-GaN/n-AlGaIn/p-AlGaIn structures can be used to modify the emission polarization, which is of interest for optimizing the extraction efficiency in NW UV LEDs.

Acknowledgments

This work was supported by the French ANR agency under the programs ANR-08-BLAN-0179 NanoPhotoNit. GJ acknowledges financial support from the Ministère de l'Enseignement Supérieur et de la Recherche.

References

[1] Vilhunen S, Särkkä H and Sillanpää M 2009 *Environ. Sci. Pollut. Res.* **16** 439–42

- [2] Morison W L 2005 *Phototherapy and Photochemotherapy of Skin Disease* (Boca Raton, FL: Taylor and Francis)
- [3] Hirayama H, Tsukada Y, Maeda T and Kamata N 2010 *Appl. Phys. Express* **3** 031002
- [4] Kneissl M et al 2011 *Semicond. Sci. Technol.* **26** 014036
- [5] Nakarmi M L, Kim K H, Khizar M, Fan Z Y, Lin J Y and Jiang H X 2005 *Appl. Phys. Lett.* **86** 092108
- [6] Nishida T, Saito H and Kobayashi N 2001 *Appl. Phys. Lett.* **78** 399
- [7] Khizar M, Fan Z Y, Kim K H, Lin J Y and Jiang H X 2005 *Appl. Phys. Lett.* **86** 173504
- [8] Atsushi Yamaguchi A 2010 *Appl. Phys. Lett.* **96** 151911
- [9] Smith G A 2004 *J. Appl. Phys.* **95** 8247
- [10] Dong Y, Tian B, Kempa T J and Lieber C M 2009 *Nano Lett.* **9** 2183–7
- [11] Qian F, Gradecak S, Li Y, Wen C Y and Lieber C M 2005 *Nano Lett.* **5** 2287–91
- [12] Jacopin G et al 2012 *Appl. Phys. Express* **5** 014101
- [13] Fang Qian Y L, Li Y, Gradecak S, Park H-G, Dong Y, Ding Y, Wang Z L and Lieber C M 2008 *Nature Mater.* **7** 701–6
- [14] Hersee S D, Rishinaramangalam A K, Fairchild M N, Zhang L and Varangis P 2011 *J. Mater. Res.* **26** 2293–8
- [15] Bertness K A, Sanford N A and Davydov A V 2011 *IEEE J. Sel. Top. Quantum* **17** 847
- [16] Schlager J B, Bertness K A, Blanchard P T, Robins L H, Roshko A and Sanford N A 2008 *J. Appl. Phys.* **103** 124309
- [17] Rigutti L, Jacopin G, Largeau L, Galopin E, De Luna Bugallo A, Julien F H, Harmand J-C, Glas F and Tchernycheva M 2011 *Phys. Rev. B* **83** 155320
- [18] Chen H Y, Yang Y C, Lin H W, Chang S C and Gwo S 2008 *Opt. Express* **16** 13465–75
- [19] Ruda H E and Shik A 2006 *J. Appl. Phys.* **100** 024314
- [20] Chuang S and Chang C 1996 *Phys. Rev. B* **54** 2491–504
- [21] Bertness K, Roshko A, Mansfield L, Harvey T and Sanford N 2007 *J. Cryst. Growth* **300** 94–9
- [22] Sanders A et al 2011 *Nanotechnology* **22** 465703
- [23] Sanford A, Robins L H, Davydov A V, Shapiro A, Tsvetkov D V, Dmitriev A V, Keller S, Mishra U K and DenBaars S P 2003 *J. Appl. Phys.* **94** 2980
- [24] Drouin D, Couture A R, Joly D, Tastet X, Aimez V and Gauvin R 2007 *Scanning* **29** 92–101
- [25] Reshchikov M A and Morkoç H 2005 *J. Appl. Phys.* **97** 061301
- [26] Li R et al 2009 *Appl. Phys. Lett.* **94** 211103
- [27] Calleja E, Sánchez-García M, Sánchez F, Calle F, Naranjo F, Muñoz E, Jahn U and Ploog K 2000 *Phys. Rev. B* **62** 16826–34
- [28] Ghosh S, Waltereit P, Brandt O, Grahn H and Ploog K 2002 *Phys. Rev. B* **65** 075202
- [29] Vurgaftman I and Meyer J R 2003 *J. Appl. Phys.* **94** 3675
- [30] Yun F, Reshchikov M A, He L, King T, Morkoç H, Novak S W and Wei L 2002 *J. Appl. Phys.* **92** 4837
- [31] Ruda H E and Shik A 2006 *J. Appl. Phys.* **100** 024314
- [32] Rigutti L et al 2010 *Phys. Rev. B* **81** 045411
- [33] Hestroffer K et al 2010 *Nanotechnology* **21** 415702
- [34] Laneuville V et al 2011 *Phys. Rev. B* **83** 115417
- [35] Raychaudhuri S and Yu E T 2006 *J. Appl. Phys.* **99** 114308
- [36] Gil B, Briot O and Aulombard R-L 1995 *Phys. Rev. B* **52** R17028
- [37] Atsushi Yamaguchi A 2008 *Phys. Status Solidi c* **5** 2364–6